

Desynchronization of strongly nonlinear oscillations by coupling's strengthening

Idan Sorin and Alexander Nepomnyashchy

*Department of Mathematics, Technion–Israel Institute of Technology,
Haifa 32000, Israel*

December 1, 2025

Abstract

We investigate cyclic dominance models and their extensions to both network systems and reaction–diffusion frameworks. Through linear stability analysis, we establish the relationship between the stability of synchronized states in networked systems and the response of homogeneous solutions subjected to spatially periodic perturbations. Furthermore, we explore the mathematical properties of networks characterized by strong nonlinear oscillations in an ecological context. Finally, we present numerical results for the master stability function of a competitive three-species Lotka–Volterra model, highlighting its role in understanding the dynamics of cyclic competition.

Keywords: Networks, Instability, Lotka–Volterra model, Synchronization, Floquet theory

1 Introduction

In [1], it was shown that spatially uniform periodic oscillations become generically unstable with respect to a spatially periodic modulation, when they approach a homoclinic bifurcation. Two instability scenarios have been revealed. Due to the invariance of an autonomous problem with respect to a time shift, one of the Floquet multipliers for spatially uniform disturbances with the wavenumber $k = 0$ is equal to 1. Within the first instability scenario, that multiplier becomes larger than 1 for arbitrary small values of k , generating a long-wave phase instability. For the second kind of instability, one of the multipliers becomes smaller than -1 in a finite interval $k_{min} < k < k_{max}$, which corresponds to a period-doubling instability combined with the creation of oscillating spatial patterns.

Recently, the period-doubling instability that breaks the spatial uniformity of the solution was found for oscillations in the spatially extended May–Leonard model [2], where a continuum of time-periodic solutions coexists with a robust heteroclinic cycle [3]. Similarly to the problem considered in [1], an instability with respect to spatially periodic modulation combined with period doubling was found in a finite interval of wavenumbers for long-period oscillations close to the heteroclinic cycle.

In the present paper, we show that the instability in spatially continuous systems discussed above has a counterpart in discrete networks of strongly nonlinear oscillators. In a continuous system, the instability takes place in a finite interval of wavenumber values; in networks, this desynchronizing instability takes place in finite intervals of values of the coupling constant. Thus, the synchronous oscillations are stable for both weak and strong couplings but are destroyed in finite intervals of the coupling constant values. Section 2 contains a description of the basic definitions and relevant properties of spatially extended systems and oscillator networks. In Section 3, our basic example, the competitive Lotka–Volterra model, and its extensions are described. In Section 4, we consider the stability of synchronous oscillations and demonstrate the similarity between the period-doubling bifurcation forming spatial patterns in a continuously extended Lotka–Volterra model and desynchronization of oscillations in non-directed networks characterized by a symmetric coupling matrix. Section 5 is devoted to the general case of an asymmetric coupling matrix, which can have complex eigenvalues. Section 6 contains concluding remarks.

2 Models of nonlinear oscillations and their extensions

2.1 ODE models

The standard way to describe a nonlinear oscillator is to present the system of ODEs governing its dynamics,

$$\frac{du_i}{dt} = f_i(u_1, \dots, u_n), \quad i = 1, \dots, n; \quad 0 < t < \infty, \quad (1)$$

where $u_1(t), \dots, u_n(t)$ are functions of time that determine the temporal evolution of the state, and f_i are generally nonlinear functions characterizing interactions within the system (“reaction terms”). Those functions may also depend on a set of parameters r_1, \dots, r_s . Later on, we assume that for some values of these parameters, the system has a time-periodic solution $u_1^{(0)}(t), \dots, u_n^{(0)}(t)$ with a period T . Because the system is autonomous, there exists a family of periodic solutions $u_1^{(0)}(t+\tau), \dots, u_n^{(0)}(t+\tau)$, where τ is an arbitrary constant in the interval $0 \leq \tau < T$.

2.2 Reaction-diffusion extension

A typical extension of the ODE system (1) is the PDE system, which takes into account a nonuniform spatial distribution of variables and their diffusion:

$$u_{it} = f_i(u_1, \dots, u_n) + d_i u_{ixx}, \quad i = 1, \dots, n; \quad 0 < t < \infty; \quad -\infty < x < \infty. \quad (2)$$

The variables u_i now depend both on the temporal coordinate t and on the spatial coordinate x . The subscripts t and x mean the partial derivatives with respect to the corresponding variables. The diffusion terms describe the spread of the component densities u_i along the axis x . The system (2) has a class of solutions that do not depend on x and satisfy the system (1). Denote the spatially uniform time-periodic solution of equations (2) and (1) with a certain time period T as $u_i^{(0)}(t)$. It is significant that this solution can be stable within the ODE system (1) and unstable within the framework of the PDE system (2) with respect to spatially non-uniform disturbances. To investigate the linear stability of that solution, one considers the evolution of a small periodic disturbance:

$$u_i(x, t) = u_i^{(0)}(t) + \epsilon U_i(t) e^{ikx}. \quad (3)$$

Here $0 < \epsilon \ll 1$ is a small parameter and k is the wavenumber of the disturbance. Substituting (3) into (2) and linearizing the equations obtained, one arrives at the linear system of ODEs:

$$\frac{dU_i}{dt} = \sum_{p=1}^n \left(\frac{\partial f_i}{\partial u_p} \right)_0 U_p - d_i k^2 U_i \quad (4)$$

where

$$\left(\frac{\partial f_i}{\partial u_p} \right)_0 = \left. \left(\frac{\partial f_i}{\partial u_p} \right) \right|_{u_p=u_p^{(0)}(t)} \quad (5)$$

are time-periodic functions. Thus, (4) is a linear system of ODEs with periodic coefficients. According to Floquet theory, a periodic solution is unstable if at least one of the Floquet multipliers has a modulus greater than 1.

2.3 Extension to network

The oscillators governed by equation (1) can be coupled to a network and interact with each other. Later on, we shall consider the case of linear coupling between identical oscillators:

$$\frac{du_{ij}}{dt} = f_i(u_{1j}, \dots, u_{nj}) + D_i \sum_{l=1}^m C_{jl} u_{il}, \quad (6)$$

$i = 1, \dots, n$, $j = 1, \dots, m$, where i is the number of the component and j is the number of the node. Later on, we shall assume that the coupling matrix C corresponds to a certain kind of generalized diffusion between the nodes of the network, and therefore it satisfies the condition of zero sum [4]:

$$\sum_{l=1}^m C_{jl} = 0. \quad (7)$$

In that case, the oscillatory subsystems can perform *synchronous* oscillations

$$u_{i1}(t) = \dots = u_{im}(t) = u_i^{(0)}(t). \quad (8)$$

The evolution of small disturbances on the background of the periodic synchronized solution is governed by linearized equations,

$$\frac{d\tilde{u}_{ij}}{dt} = \sum_{p=1}^n \left(\frac{\partial f_i}{\partial u_p} \right)_0 \tilde{u}_{pj} + D_i \sum_{l=1}^m C_{jl} \tilde{u}_{il}, \quad (9)$$

where

$$\left(\frac{\partial f_i}{\partial u_p} \right)_0 = \left. \frac{\partial f_i}{\partial u_{pj}} \right|_{u_{pj}=u_p^{(0)}} \quad \text{for all } j.$$

Consider the eigenvalue problem,

$$\sum_{l=1}^m C_{jl} v_l = \lambda v_j, \quad j = 1, \dots, m. \quad (10)$$

Assume that all eigenvalues of (10) are distinct, $\{\lambda^s\}_{s=1}^m$, and that the eigenvectors $\{v_j^s\}$ form a basis of \mathbb{R}^m . Expand \tilde{u}_{il} with respect to this basis:

$$\tilde{u}_{il}(t) = \sum_{s=1}^m U_i^s(t) v_l^s. \quad (11)$$

Substituting (11) into (9) and using (10), we obtain:

$$\sum_{s=1}^m \frac{dU_i^s}{dt} v_j^s = \sum_{s=1}^m \sum_{p=1}^n \left(\frac{\partial f_i}{\partial u_p} \right)_0 U_p^s(t) v_j^s + D_i \sum_{s=1}^m U_i^s(t) \lambda^s v_j^s. \quad (12)$$

Since vectors $\{v_j^s\}$ form a basis, we conclude that

$$\frac{dU_i^s}{dt} = \sum_{p=1}^n \left(\frac{\partial f_i}{\partial u_p} \right)_0 U_p^s + D_i \lambda^s U_i^s. \quad (13)$$

For each s , system (13) is equivalent to the linearized system for the corresponding reaction-diffusion equation (4) with $D_i \lambda^s$ instead of $-D_i k^2$. Similar analysis can be found in [5].

For real non-positive λ^s , the results obtained by studying the instability of the spatially homogeneous oscillation in the framework of the reaction diffusion equations can be directly applied to the problem of the instability of synchronous oscillations in the network.

In biological applications, where variables are densities of species, animals can only leave a definite node or stay there, and only species from other nodes can enter that node. Within this scenario, the diagonal elements of the matrix C are non-positive and the off-diagonal elements of C are non-negative. Thus, the matrix C is a Metzler matrix [6]. Since

$$\sum_{l=1}^m C_{jl} = 0,$$

we find that

$$-C_{jj} = \sum_{j \neq l=1}^m |C_{jl}|.$$

From the Gershgorin circle theorem [7], all the eigenvalues lie inside the union of the circles:

$$|z - C_{jj}| \leq -C_{jj}.$$

If we denote $c = \min_j \{C_{jj}\}$, the circle $|z - c| \leq -c$ contains all the other circles, therefore, all the eigenvalues of the matrix C are within that circle. The eigenvalue with the largest real part of a Metzler matrix is called the Perron eigenvalue. If a Metzler matrix is irreducible, from the Perron–Frobenius theorem, this eigenvalue is simple. We assume that system (6) describes a network that is a strongly connected graph, because if this is not the case, then system (6) can be separated into nonconjugated systems that can be analyzed independently. This means that 0 is a simple eigenvalue and there are no other eigenvalues with the real part equal to zero. Now, since C is a real matrix, if λ is an eigenvalue of C , then $\bar{\lambda}$ is also an eigenvalue of C . The Floquet multipliers of system (13) with $\lambda^s = \lambda$ are the same as with $\lambda^s = \bar{\lambda}$. Therefore, in order to check the stability of the synchronized solution $u_i^{(0)}$ for a general C , it is enough to check the stability for the eigenvalues only in the second or the third quadrant of the complex plane.

Note that if we denote $h = \max\{C_{ij}, i \neq j\}$, m as the size of the matrix C , we can write $C = -hm\tilde{C}$. In this notation, \tilde{C} is called a "standardized Laplacian matrix", and its eigenvalues μ are located in the first and fourth quadrants. Those that are located inside the first quadrant satisfy $0 \leq \text{Arg}(\mu) \leq \frac{\pi}{2} - \frac{\pi}{m}$. Those eigenvalues that are located inside the fourth quadrant are just their complex conjugates [8].

Note that for networks with non-directed connections, the matrix C is symmetric and hence its eigenvalues are real. Therefore, the stability results obtained within the PDE extension provide complete information on the stability of an arbitrary network with non-directed connections.

3 Competitive Lotka-Volterra model and its extensions

As the basic model of strongly nonlinear oscillations, we consider the competitive Lotka-Volterra model, which describes the temporal evolution of n biological species competing for common resources. The dynamics is governed by the system of ODEs

$$\frac{du_i(t)}{dt} = r_i u_i(t) \left[1 - \sum_{j=1}^n \alpha_{ij} u_j(t) \right]; \quad u_i \geq 0; \quad i = 1, \dots, n. \quad (14)$$

Here $u_i(t)$ is the suitably normalized number of individuals of the i -th species at time t , r_i is the intrinsic growth rate of the i -th species, and α_{ij} are the interaction coefficients that measure the extent to which the j -th species affects the growth rate of the i -th species [9]. For $n = 3$, the system (14), after a proper rescaling, takes the form:

$$\begin{aligned} \frac{du_1}{dt} &= r_1 u_1 (1 - u_1 - \alpha_1 u_2 - \beta_1 u_3) \\ \frac{du_2}{dt} &= r_2 u_2 (1 - u_2 - \alpha_2 u_3 - \beta_2 u_1) \\ \frac{du_3}{dt} &= r_3 u_3 (1 - u_3 - \alpha_3 u_1 - \beta_3 u_2) \end{aligned} \quad (15)$$

The characteristic feature of system (15) is the existence of three invariant manifolds $u_1 = 0$, $u_2 = 0$ and $u_3 = 0$, which bound the biologically meaningful region $u_j \geq 0$, $j = 1, 2, 3$. For definite relations between the coefficient α_j and β_j , there exist heteroclinic trajectories connecting one-species saddle points in each of the manifolds, which together form a *robust* heteroclinic cycle [3, 10, 11]. In [10], it has been shown that in the case of non-equal growth rates r_i , this system can have three kinds of attractors: a coexistence state of equilibrium (none of the variables equals zero), a limit cycle, and a heteroclinic cycle. Note that in the special case $r_1 = r_2 = r_3 = r$, which is called the May-Leonard system [3], the dynamics is different: for that system, it was proven [11] that for parameters that satisfy the relation

$$(1 - \beta_1)(1 - \beta_2)(1 - \beta_3) = (\alpha_1 - 1)(\alpha_2 - 1)(\alpha_3 - 1), \quad 0 < \beta_i < 1 < \alpha_i,$$

there exists an attracting two-dimensional invariant manifold with a continuum of periodic solutions on it.

To simplify the notation, later on we denote $u \equiv u_1$, $v \equiv u_2$ and $w \equiv u_3$. As a basic example, later on we consider in detail the following two-parameter system:

$$u_t = u(\gamma - u - \alpha v), \quad (16a)$$

$$v_t = v(1 - v - \alpha w), \quad \alpha, \gamma > 0, \quad (16b)$$

$$w_t = w(1 - w - \alpha u). \quad (16c)$$

Here and below, a subscript means the derivative with respect to the corresponding variable.

This system has the coexistence solution:

$$u_* = \frac{\gamma - \alpha + \alpha^2}{1 + \alpha^3}, \quad v_* = \frac{1 - \alpha + \alpha^2 \gamma}{1 + \alpha^3}, \quad w_* = \frac{1 - \alpha \gamma + \alpha^2}{1 + \alpha^3} \quad (17)$$

We assume that

$$\alpha > 1, \quad \frac{\alpha - 1}{\alpha^2} < \gamma < \frac{\alpha^2 + 1}{\alpha}, \quad (18)$$

hence u_* , v_* , w_* are positive. With the growth of α , the coexistence solution becomes oscillatory unstable. The curve of the Hopf bifurcations that divides the stability regions of the coexistence equilibrium point and the limit cycle is determined by the relation:

$$\begin{aligned} & \alpha(1 - \alpha - \alpha^3)\gamma^3 + (-2 + 3\alpha - 5\alpha^2 + 6\alpha^3 + \alpha^5 - \alpha^6)\gamma^2 \\ & + (-4 + 7\alpha - 11\alpha^2 + 5\alpha^3 - 7\alpha^4 + \alpha^5 + \alpha^7)\gamma \\ & + (1 - \alpha)^2(-2 + \alpha - 3\alpha^2 - \alpha^3 - \alpha^4) = 0. \end{aligned} \quad (19)$$

We denote the periodic solution as

$$u(t) = u_0(t), \quad v(t) = v_0(t), \quad w(t) = w_0(t) \quad (20)$$

and its period as T . In fact, due to the symmetry with respect to the time shift, there is a continuum of periodic solutions; we choose one of them.

In addition, this system has an unstable fixed point $(0, 0, 0)$ and three saddle nodes, which are the 1-species solutions: $(\gamma, 0, 0)$, $(0, 1, 0)$, $(0, 0, 1)$. There exists a heteroclinic cycle that connects those three points. One can show [12] that the behavior of trajectories near the heteroclinic cycle is determined by the expression

$$c = (\alpha - 1)(\alpha - \gamma)(\alpha \gamma - 1)/\gamma.$$

When $c > 1$, the heteroclinic cycle is an attractor.

The attractors of the system in the parameter region $0 < \gamma < 1$ are indicated in Figure 1.

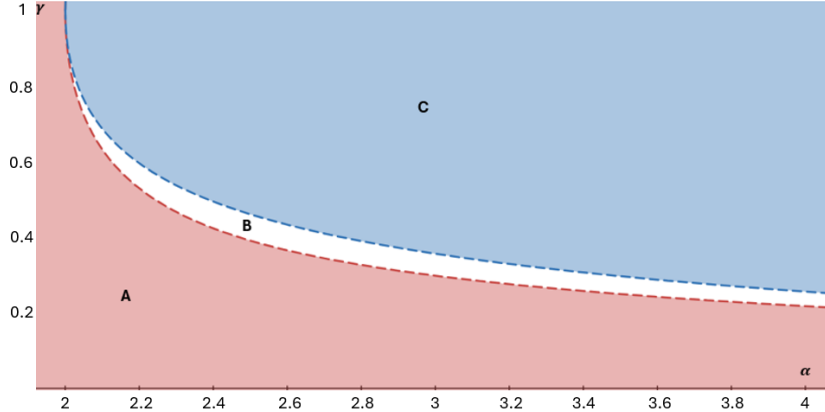


Figure 1: The parameter space (α, γ) . In region (A) the coexistence point is the attractor, in region (B) the attractor is a limit cycle, and in region (C) the attractor is a heteroclinic cycle.

In the following, we consider two types of system extensions that describe the mobility of animals.

The continuous, “reaction-diffusion”, extension of (16) is:

$$u_t = u(\gamma - u - \alpha v) + d_u u_{xx}, \quad (21a)$$

$$v_t = v(1 - v - \alpha w) + d_v v_{xx}, \quad (21b)$$

$$w_t = w(1 - w - \alpha u) + d_w w_{xx}; \quad -\infty < x < \infty. \quad (21c)$$

Here u , v and w are functions of the temporal coordinate t and the spatial coordinate x . The system (21) has a solution that does not depend on x and coincides with the solution of the ODE system discussed above:

$$u(x, t) = u_0(t), \quad v(x, t) = v_0(t), \quad w(x, t) = w_0(t), \quad (22)$$

which corresponds to synchronous oscillations throughout the space.

We shall also consider another kind of extensions, (16) to namely, the network:

$$u_j = u_j(\gamma - u_j - \alpha v_j) + D_u \sum_{l=1}^m C_{jl} u_l, \quad (23a)$$

$$v_j = v_j(1 - v_j - \alpha w_j) + D_v \sum_{l=1}^m C_{jl} v_l, \quad (23b)$$

$$\dot{w}_j = w_j(1 - w_j - \alpha u_j) + D_w \sum_{l=1}^m C_{jl} w_l. \quad (23c)$$

$j = 1, \dots, m$. The matrix $[C_{jl}]_{j,l=1}^{j,l=m}$ is called below the coupling matrix. All subsystems that make up the network are assumed to be identical, and the coupling matrix is the same for all species.

Biologically, this can be understood as m different habitats, with the same ecological system in each of them. In each habitat, the same species live with the same dynamic between them, but the animals can move from one habitat to another. Here, we assume the existence of a synchronized periodic solution with

$$u_j(t) = u_0(t), \quad v_j(t) = v_0(t), \quad w_j(t) = w_0(t) \quad (24)$$

for every $1 \leq j \leq m$. Therefore, we demand:

$$\sum_{l=1}^m C_{jl} = 0 \quad (25)$$

which means that the sum of every row in the connectivity matrix is zero.

4 Instabilities of synchronous oscillations

As mentioned above, while the periodic solution (20) is stable in the framework of the system (16), its spatial extension (22) and network extension (24) can be unstable with respect to desynchronizing disturbances. This phenomenon is considered in the present section.

4.1 The case of spatial extension

As in (3), we add a small disturbance to the time-periodic solution (20):

$$(u, v, w) = (u_0(t) + \epsilon U(t)e^{ikx}, v_0(t) + \epsilon V(t)e^{ikx}, w_0(t) + \epsilon W(t)e^{ikx}), \quad 0 < \epsilon \ll 1, \quad (26)$$

so that the linearized system is:

$$\begin{pmatrix} \dot{U} \\ \dot{V} \\ \dot{W} \end{pmatrix} = - \begin{pmatrix} d_u k^2 - \gamma + 2u_0(t) + \alpha v_0(t) & \alpha u_0(t) & 0 \\ 0 & d_v k^2 - 1 + 2v_0(t) + \alpha w_0(t) & \alpha v_0(t) \\ \alpha w_0(t) & 0 & d_w k^2 - 1 + 2w_0(t) + \alpha u_0(t) \end{pmatrix} \begin{pmatrix} U \\ V \\ W \end{pmatrix}. \quad (27)$$

In the following, we set $\gamma = 0.5$, $d_u = 1$, $d_v = d_w = 0$, and choose α in the region (B) of Figure 1, $\alpha_- < \alpha < \alpha_+$, where $\alpha_- \approx 2.24$, $\alpha_+ \approx 2.38$.

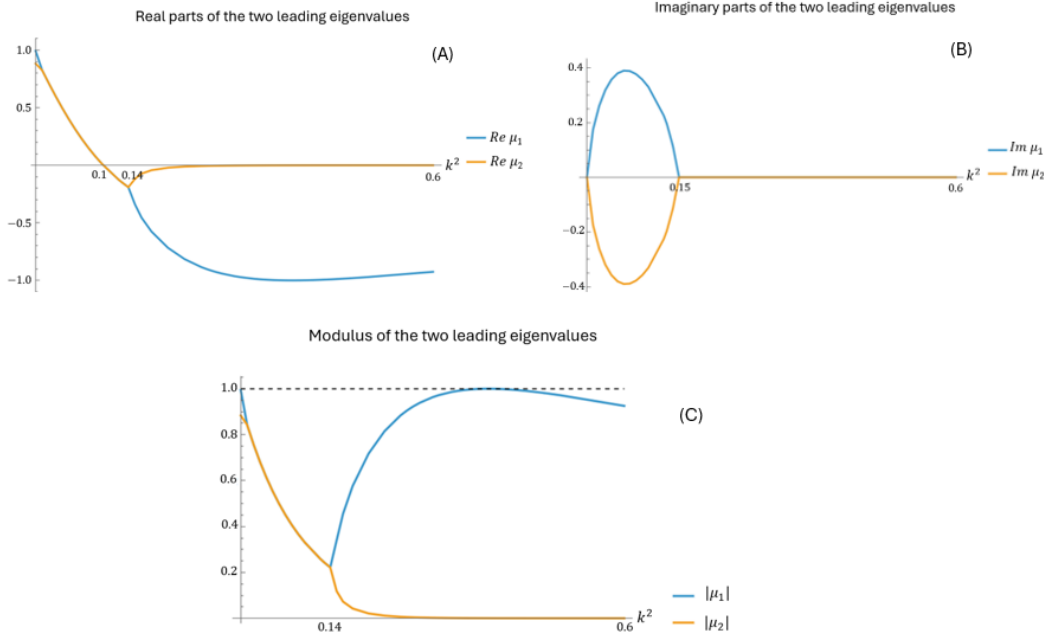


Figure 2: Period doubling at a finite wavenumber for $d_u = 1, d_v = d_w = 0$. In (A),(B),(C) the Real, Imaginary, and Modulus of the two leading eigenvalues are shown respectively at $\alpha = 2.3427$.

Integrating (27) within the interval $0 \leq t \leq T$ for three linearly independent initial conditions, we obtain the monodromy matrix $\mathbf{M}(k^2)$ that relates the vectors $(U(T), V(T), W(T))^T$ and $(U(0), V(0), W(0))^T$:

$$\begin{pmatrix} U(T) \\ V(T) \\ W(T) \end{pmatrix} = \mathbf{M}(k^2) \begin{pmatrix} U(0) \\ V(0) \\ W(0) \end{pmatrix}. \quad (28)$$

The eigenvalues $\mu_i, i = 1, 2, 3$, of the monodromy matrix (multipliers) determine the stability of the solution (20).

The results of the multiplier calculation for $\alpha = 2.3427$ are shown in Figure 2. One of the multipliers is always very close to zero; it is irrelevant and is not presented in the plots. For the other two multipliers, $\text{Re}\mu_i$, $\text{Im}\mu_i$, and $|\mu_i|$ are shown as functions of k^2 . Note that there is a small interval near k^2 where the multipliers are real. This interval cannot be seen in the graphs due to resolution issues. At $k^2 = 0$, one of the multipliers is equal to 1 (it corresponds to the time shift) and another is positive and smaller than 1, which confirms the stability of solution (20) in the framework of the system (16). At small k^2 , both multipliers are positive and smaller than 1; that means that synchronous oscillations are stable with respect to spatially periodic disturbances. There is a certain $\alpha = \alpha_*$, such that at $\alpha < \alpha_*$, $|\mu(k^2)| < 1$ for all multipliers for any $k^2 \neq 0$, that is, the spatially uniform solution is stable. However, at $\alpha > \alpha_*$, $\mu(k^2) < -1$ in a certain interval $k_{min}^2 < k^2 < k_{max}^2$. That means that within that interval the multiplier $\mu(k^2)$ crosses the value -1, creating the instability with respect to oscillations with period $2T$ and periodic in space with period $2\pi/k$. We find the critical value $\alpha = \alpha_* \approx 2.34$, and for that value $\mu(k^2) = -1$ at $k = k_* \approx 0.62$. Thus, the temporal period of the critical disturbance is twice as large as that of the basic oscillation (see Figure 3). One can expect that the instability described above leads to the appearance of a spatially periodic solution with a double temporal period. This assumption is confirmed by numerical simulations of system (23), which are not presented here.

The instability described above is similar to that found in [2] for periodic solutions of the May-Leonard system close to the heteroclinic cycle. Another example of this instability is given in [1].

Note that with a further growth of α , the time-periodic oscillations are replaced by quasiperiodic oscillations due to a secondary instability. The analysis of secondary bifurcations is beyond the scope of this paper.

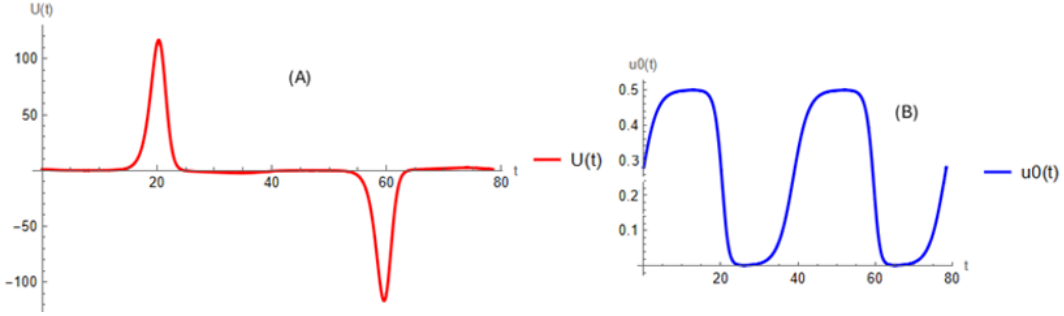


Figure 3: Period doubling at finite wavenumber for $d_u = 1, d_v = d_w = 0$. (A) The disturbance with $k = k_*$ at $\alpha = 2.3427$. Its period is twice the period of the base solution (B).

4.2 The case of network extension

Consider now the network (23). Linearizing equations (23) around the periodic solution (24) corresponding to synchronous oscillations, we obtain for disturbances $(U_j(t), V_j(t), W_j(t))$, $j = 1, \dots, m$:

$$\dot{U}_j = (\gamma - 2u_0 - \alpha v_0)U_j - \alpha u_0 V_j + D_u \sum_{l=1}^m C_{jl} U_l, \quad (29a)$$

$$\dot{V}_j = (1 - 2v_0 - \alpha w_0)V_j - \alpha v_0 W_j + D_v \sum_{l=1}^m C_{jl} V_l, \quad (29b)$$

$$\dot{W}_j = -\alpha w_0 U_j + (1 - 2w_0 - \alpha u_0)W_j + D_w \sum_{l=1}^m C_{jl} W_l, \quad (29c)$$

$$j = 1, \dots, m.$$

As explained in section 2.3, the expansion of vectors (U_j, V_j, W_j) over the eigenvectors of the coupling matrix C splits the system (29) of order $3m$ into m decoupled systems equivalent to (27) with $-d_u k^2, -d_v k^2, -d_w k^2$ replaced with $D_u \lambda^s, D_v \lambda^s, D_w \lambda^s$, where $\{\lambda^s\}$, $s = 1, \dots, m$, are the eigenvalues of matrix C .

Before studying the general case, consider several particular cases.

4.2.1 Two coupled subsystems

First, let us consider the simplest “network” that consists of two coupled subsystems,

$$\dot{u}_1 = u_1(\gamma - u_1 - \alpha v_1) + D(u_2 - u_1), \quad \dot{v}_1 = v_1(1 - v_1 - \alpha w_1), \quad \dot{w}_1 = w_1(1 - w_1 - \alpha u_1), \quad (30)$$

$$\dot{u}_2 = u_2(\gamma - u_2 - \alpha v_2) + D(u_1 - u_2), \quad \dot{v}_2 = v_2(1 - v_2 - \alpha w_2), \quad \dot{w}_2 = w_2(1 - w_2 - \alpha u_2), \quad (31)$$

which has the synchronized basic solution

$$u_1 = u_2 = u_0(t), \quad v_1 = v_2 = v_0(t), \quad w_1 = w_2 = w_0(t).$$

Its stability is determined by the system

$$\begin{aligned} \dot{U}_1 &= U_1(\gamma - 2u_0 - \alpha v_0 - D) - \alpha u_0 V_1 + D U_2, & \dot{V}_1 &= V_1(1 - 2v_0 - \alpha w_0) - \alpha v_0 W_1, \\ \dot{W}_1 &= W_1(1 - 2w_0 - \alpha u_0) - \alpha w_0 U_1, \end{aligned} \quad (32)$$

$$\begin{aligned} \dot{U}_2 &= U_2(\gamma - 2u_0 - \alpha v_0 - D) - \alpha u_0 V_2 + D U_1, & \dot{V}_2 &= V_2(1 - 2v_0 - \alpha w_0) - \alpha v_0 W_2, \\ \dot{W}_2 &= W_2(1 - 2w_0 - \alpha u_0) - \alpha w_0 U_2, \end{aligned} \quad (33)$$

Define

$$U_{\pm} = U_1 \pm U_2, \quad V_{\pm} = V_1 \pm V_2, \quad W_{\pm} = W_1 \pm W_2.$$

Then

$$\begin{aligned}\dot{U}_+ &= U_+(\gamma - 2u_0 - \alpha v_0) - \alpha u_0 V_+, \quad \dot{V}_+ = V_+(1 - 2v_0 - \alpha w_0) - \alpha v_0 W_+, \\ \dot{W}_+ &= W_+(1 - 2w_0 - \alpha u_0) - \alpha w_0 U_+, \end{aligned}\tag{34}$$

$$\begin{aligned}\dot{U}_- &= U_-(\gamma - 2u_0 - \alpha v_0 - 2D) - \alpha u_0 V_-, \quad \dot{V}_- = V_-(1 - 2v_0 - \alpha w_0) - \alpha v_0 W_-, \\ \dot{W}_- &= W_-(1 - 2w_0 - \alpha u_0) - \alpha w_0 U_-. \end{aligned}\tag{35}$$

Equations (34) and (35) are equivalent to (27) with $k^2 = 0$ and $d_u k^2 = 2D$, respectively. Therefore, there exist two branches of multipliers: one with constant multipliers,

$$\mu_j^+(D) = \mu_j(0), \quad j = 1, 2, 3,$$

equal to the multipliers of problem (27) at $k^2 = 0$ and a branch

$$\mu_j^-(D) = \mu_j(2D/d_u), \quad j = 1, 2, 3,$$

and another with multipliers equal to the multipliers of the problem (27) at

$$k^2 = 2D/d_u. \tag{36}$$

The plot of $\mu_j^-(D)$ for the desynchronization mode is equivalent to that shown in Figure 2 with replacement (36).

At $\alpha > \alpha_*$, $\alpha_* \approx 2.34$, the instability of synchronous oscillations takes place in the interval of the values of the coupling constant $D_- < D < D_+$, where $D_{\pm} = d_u k_{\pm}^2(\alpha)/2$. It is interesting that synchronous oscillations are *stable* at sufficiently small D , $0 < D < D_-$, and are desynchronized with the *growth* of the coupling constant D above D_- . At $D > D_+$, the synchronous oscillations become stable again.

Note that desynchronization by strengthening the coupling constant was observed in [16].

The period-doubling bifurcation in the two-site system is shown in Figure 4. Figure 4B shows the dependence $|\mu(D)|$ for the multiplier with the highest modulus value. Figure 4A demonstrates the oscillations with the double period obtained by numerical simulation of the system (30), (31).

In the regions of linear stability of synchronous oscillations, the numerical simulation shows that there is a synchronization of oscillations in both subsystems for different initial conditions. In Figure 5, it can be seen how system (30), (31) with different initial conditions of $u_1(t), u_2(t)$ is synchronized to a periodic solution with $u_1(t) = u_2(t), v_1(t) = v_2(t), w_1(t) = w_2(t)$.

4.2.2 Networks with real eigenvalues

Now, consider a network of more than two coupled subsystems, but assuming that all the eigenvalues of the matrix C are real and negative. This is always the case when C is symmetric and Metzler. It was shown that one of the eigenvalues is zero and the others are strictly negative.

Assume that for a set of parameters (d_u, d_v, d_w, k) , the stability analysis for the PDE model (21) predicts the instability in a certain interval $k_{min} < k < k_{max}$. Let us consider system (29) and start changing D_u , D_v and D_w proportionally keeping constant the ratios $D_v/D_u = d_v/d_u$, $D_w/D_u = d_w/d_u$. For each eigenvalue $\lambda^s < 0$, $s = 1, \dots, n$, of the matrix C , three multipliers of system (29) for a definite D_u coincide with three multipliers of system (27) at the value of k satisfying the relation $D_u \lambda^s = -d_u k^2$. Thus, for each λ^s , there will be instability in the interval $-d_u k_{min}^2/\lambda^s < D_u < -d_u k_{max}^2/\lambda^s$.

When two eigenvalues $\lambda^{s_1}, \lambda^{s_2}$ are close enough, their instability intervals will intersect, generating a larger instability interval. When the eigenvalues of the matrix C are far enough, there will be separate instability intervals.

An example of this phenomenon with the matrix $C = \begin{bmatrix} -3 & 1 & 2 \\ 1 & -2 & 1 \\ 2 & 1 & -3 \end{bmatrix}$ can be seen in Figure 6.

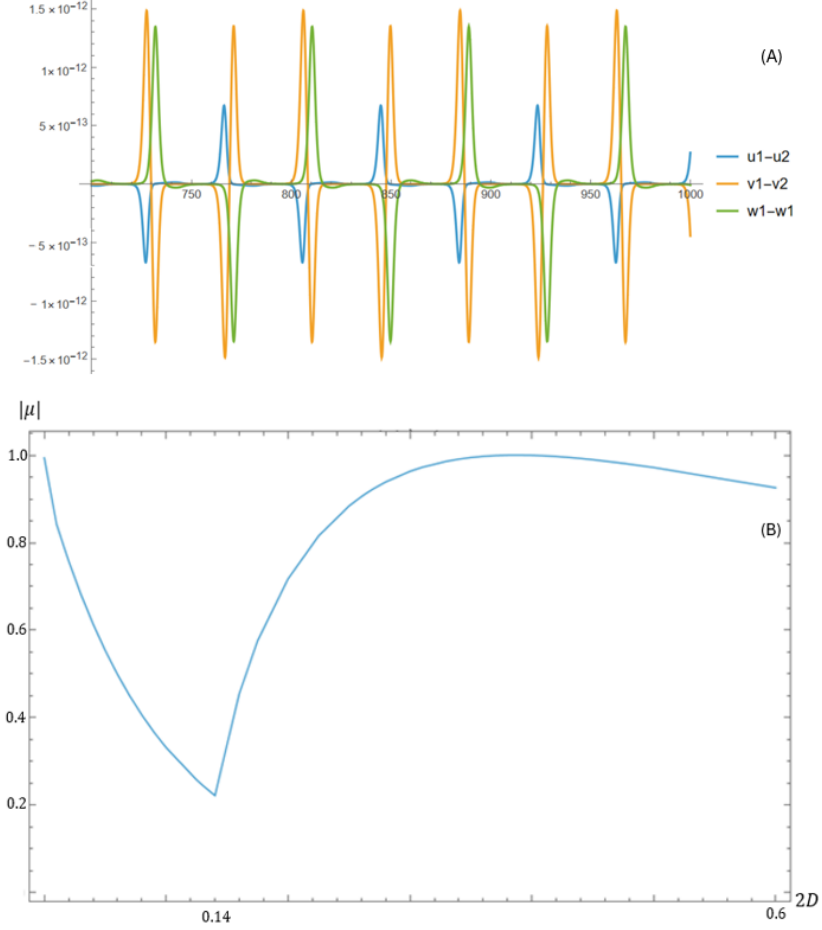


Figure 4: Period doubling bifurcation in the network with the two coupled subsystems (A) and its corresponding Floquet multiplier (B). Similarly to Fig.2, $\alpha = 2.3427$, $\gamma = 0.5$, $D = k_*^2/2 = 0.1922$.

4.2.3 Networks with complex eigenvalues

We now consider the case where the matrix C has a pair of complex eigenvalues λ^s and $\bar{\lambda}^s$. That may happen in the case of a directed network with a non-symmetric coupling matrix. Note that now the stability results obtained within the PDE extension cannot provide the complete information about the stability of the network system, since the wavenumbers k are real. It was shown that when C is a Metzler matrix, with sum zero of each row λ^s must be inside the left half of the complex plane, hence it is sufficient to look at λ^s only in the second or third quadrant.

In the following, we assume that $D_u \neq 0$. We are interested in finding the multipliers for the system

$$\dot{U}^s = (\gamma - 2u_0 - \alpha v_0)U^s - \alpha u_0 V^s + D_u \lambda^s U^s, \quad (37)$$

$$\dot{V}^s = (1 - 2v_0 - \alpha w_0)V^s - \alpha v_0 W^s + D_v \lambda^s V^s, \quad (38)$$

$$\dot{W}^s = -\alpha w_0 U^s + (1 - 2w_0 - \alpha u_0)W^s + D_w \lambda^s W^s \quad (39)$$

as functions of $\Omega \equiv D_u \lambda^s$, while keeping constant ratios D_v/D_u and D_w/D_u .

First, consider the case of small $|\Omega|$. According to the Floquet theorem, the monodromy matrix has the form $M = \exp(\Lambda T)$, where T is the period of the solution (u_0, v_0, w_0) . For our problem, we know that at $\lambda^s = 0$, the matrices M and Λ have distinct real eigenvalues, $\mu_i = \exp(\Lambda_i T)$, $i = 1, 2, 3$. The largest multiplier $\mu_1(0) = 1$ and the growth rate $\Lambda_1(0) = 0$ correspond to the mode of translation along t . For small real negative Ω , it is known from the analysis of the PDE with $d_u k^2 = -\Omega$ that the largest multiplier $\mu_1(\Omega) < 1$ and the corresponding growth rate $\Lambda_1(\Omega) < 0$. This means, that μ_1 can be expanded to a power series: $\mu_1 = 1 + a_1 \Omega + O(\Omega^2)$, $a_1 < 0$. When Ω is complex but $\text{Im}\Omega$ is small,

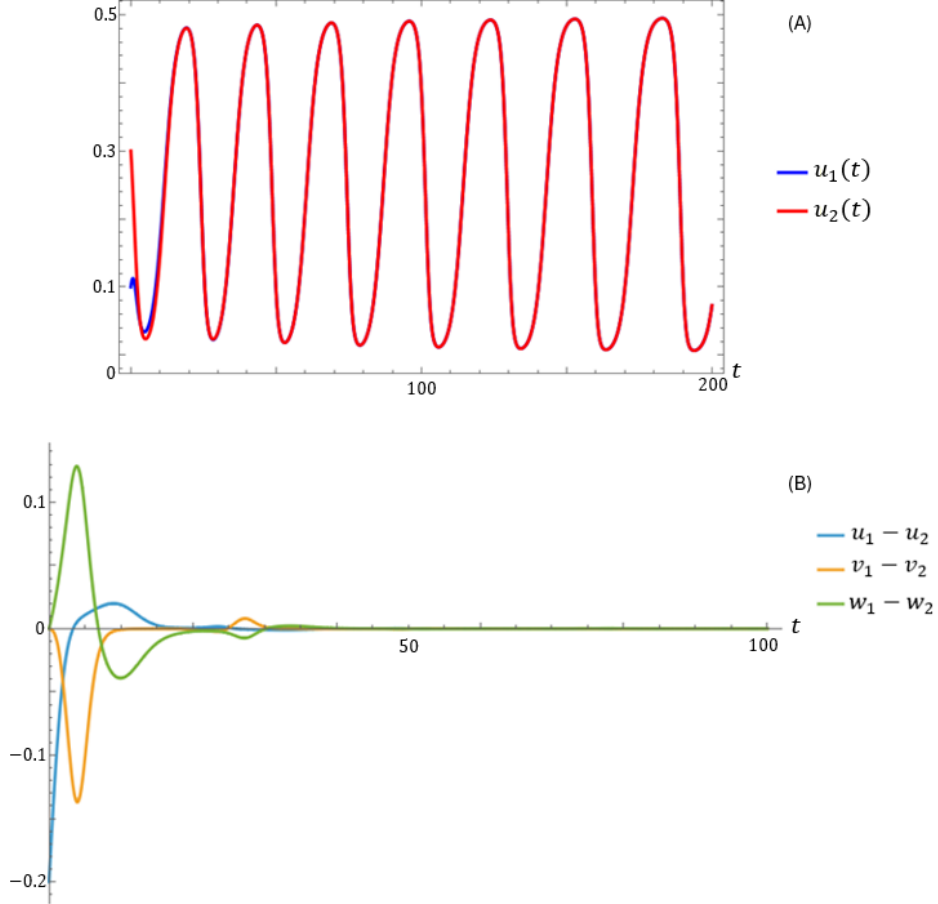


Figure 5: Synchronization between the two subsystems. $u_1(t), u_2(t)$ as a function of time (A) and the differences $u_1 - u_2, v_1 - v_2, w_1 - w_2$, as a function of time (B). $\alpha = 2.4327, \gamma = 0.5, D = 0.15, (u_1(0), v_1(0), w_1(0)) = (0.1, 0.15, 0.05), (u_2(0), v_2(0), w_2(0)) = (0.3, 0.15, 0.05)$.

due to the continuous dependence of the distinct eigenvalues of the matrix Λ on λ^s , we come to the conclusion that for sufficiently small negative $\text{Re}(\Omega)$,

$$\text{Re}(\Lambda_1(\Omega)) < 0,$$

hence the modulus of the multiplier,

$$|\mu_1(\Omega)| = |\exp(\Lambda_1(\Omega))| = \exp(\text{Re}(\Lambda_1(\Omega))) < 1.$$

Thus, there is no desynchronizing instability for sufficiently small $\text{Re}(\Omega) < 0$ and $\text{Im}(\Omega) < 0$. In other words, if the stability analysis carried out for the continuous spatial extension of the problem based on system (4) predicts the absence of a long-wave modulational instability, then the synchronous oscillations in any network of the kind (6), (7) are stable at sufficiently weak coupling.

Later on, we will base our numerical results on the case $\alpha = 2.3427$, which is close to α_* , and $D_v = D_w = 0$, with the notation $D_u = D$. Fix $\lambda^s = -|\lambda^s|e^{i\theta}$ and calculate the multipliers as functions of D .

Similarly to the instability that occurs with real eigenvalues, the synchronized solution is also stable for weak and strong coupling. When θ is small enough, $|\mu_1|_{(D)}$ has only one minimum and one maximum, as in Figure 2, which means that there is an interval of D for which the synchronized solution is unstable. When θ crosses a critical value, $|\mu_1|_{(D)}$ has an inflection point that is split into a minimum and maximum point as θ increases. At this stage, $|\mu_1|_{(D)}$ is greater than 1. After increasing θ more, the minimum point is below $|\mu_1|_{(D)}=1$ and the maximum point has a higher value of $|\mu_1|_{(D)}$. These cases can be seen in Figure 7.

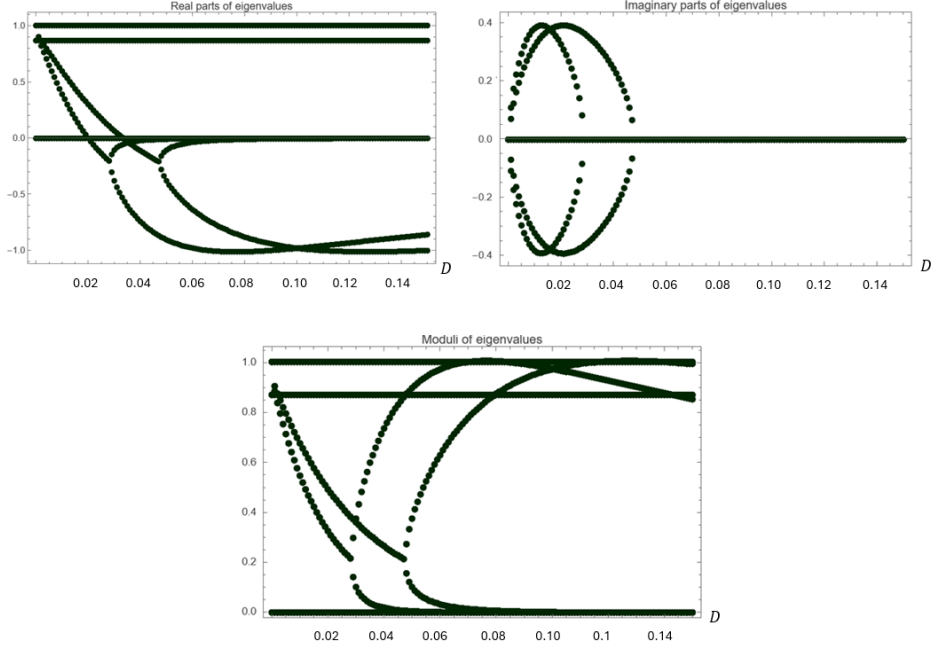


Figure 6: Floquet multipliers, with the eigenvalues $\{-5, -3, 0\}$. $\alpha = 2.3435$, $\gamma = 0.5$, $D_u = D$, $D_v = D_w = 0$.

In the $\theta \neq 0$ case, the imaginary part of $\mu_{1(D)}$ is generally not zero, meaning that instead of the period-doubling bifurcation, there is a quasi-periodic bifurcation. In Figure 8, quasiperiodic oscillations of $u_1(t) - u_2(t)$ are demonstrated that have been simulated right above the instability threshold. Let us note that this case has no analog for reaction-diffusion systems or non-directed networks with symmetric coupling matrices. The quasi-periodic behavior follows from the Floquet multipliers. The absolute value of one of them, μ_1 , first crosses 1 while its imaginary part is not zero. Now, the solution has the form:

$$u_j(t) = u_0(t) + \epsilon \sum_{n,m \in \mathbb{Z} \setminus \{0\}} A_{n,m}^{(j)} e^{i(n\omega_1 + m\omega_2)t}$$

(and similarly for v_j, w_j). Therefore, the bifurcation can be seen clearly from the Fourier transform of $u_1(t) - u_2(t)$: $\mathcal{F}[u_1(t) - u_2(t)](\omega)$, which shows that there are two basic frequencies. These frequencies can be calculated directly from the solutions of the uncoupled system (22) and the Floquet multipliers by the formula: $\omega_1 = 2\pi/T$, $\omega_2 = \text{Arg}(\mu_1)/T$, where T is the period of (22). Numerically, we find $\omega_1 \approx 0.16$, $\omega_2 \approx 0.019$. Since the order-zero terms diminish in the subtraction $u_1(t) - u_2(t)$, we would expect to see peaks in the frequencies which have the form (approximately) $n\omega_1 + m\omega_2$, and indeed the biggest peaks are in $\omega_1 \pm \omega_2$, then in $2\omega_1 \pm \omega_2$, then in $3\omega_1 \pm \omega_2$, etc. The other combinations can also be seen, but their amplitudes are much smaller.

4.2.4 The case of Jordan block

Consider the case where C is not diagonalizable and thus has a Jordan form. In this case, the solutions of (12) can be expanded as a linear combination of the Jordan basis. Here, equation (12) has the form:

$$\sum_{s=1}^m \frac{dU_i^s}{dt} v_j^s = \sum_{s=1}^m \sum_{p=1}^n \left(\frac{\partial f_i}{\partial u_p} \right)_0 U_p^s(t) v_j^s + D_i \sum_{s=1}^m U_i^s(t) (\lambda^s v_j^s + v_{j-1}^s), \quad (40)$$

where v_{j-1}^s is the previous vector in v_j^s 's Jordan block and is defined as zero if v_j^s is the first vector in the block or belongs to a block of size 1. Therefore, if the PDE model has an instability for a wave-number k , the network also has an instability because by choosing $D_i \lambda^s = -d_i k^2$, the corresponding linearized equation for the first vector in λ^s 's Jordan block is identical to the PDE's linearized equation, so the instability occurs also for such networks.

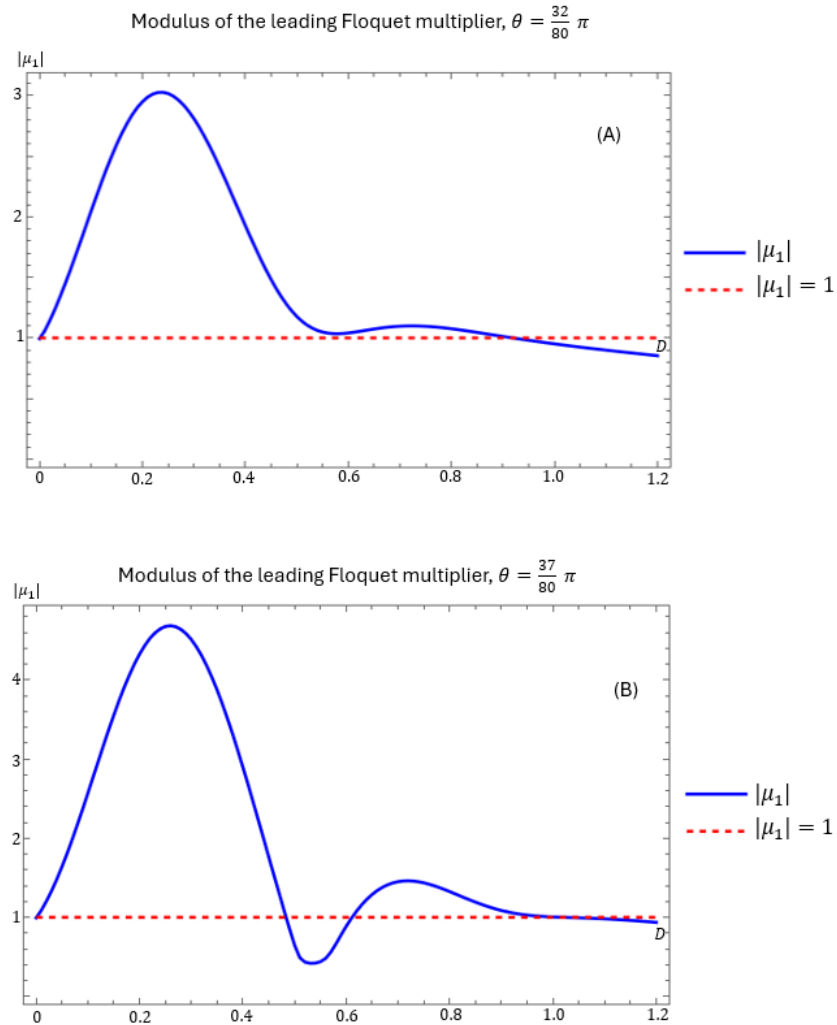


Figure 7: Absolute value of the leading Floquet Multiplier $|\mu_1|$ with (A) $\theta = \frac{33}{80} \pi$ and (B) $\theta = \frac{37}{80} \pi$. In (A) the minimum point is located above the line $|\mu_1| = 1$ and therefore there is one instability interval at $\epsilon < D < 0.92$ (ϵ is small and cannot be seen in the figure) and in (B) the minimum point is located below $|\mu_1| = 1$ and therefore there are two intervals of instability: $\epsilon^* < D < 0.49 \cup 0.61 < D < 1.04$ (ϵ^* is small and cannot be seen in the figure).

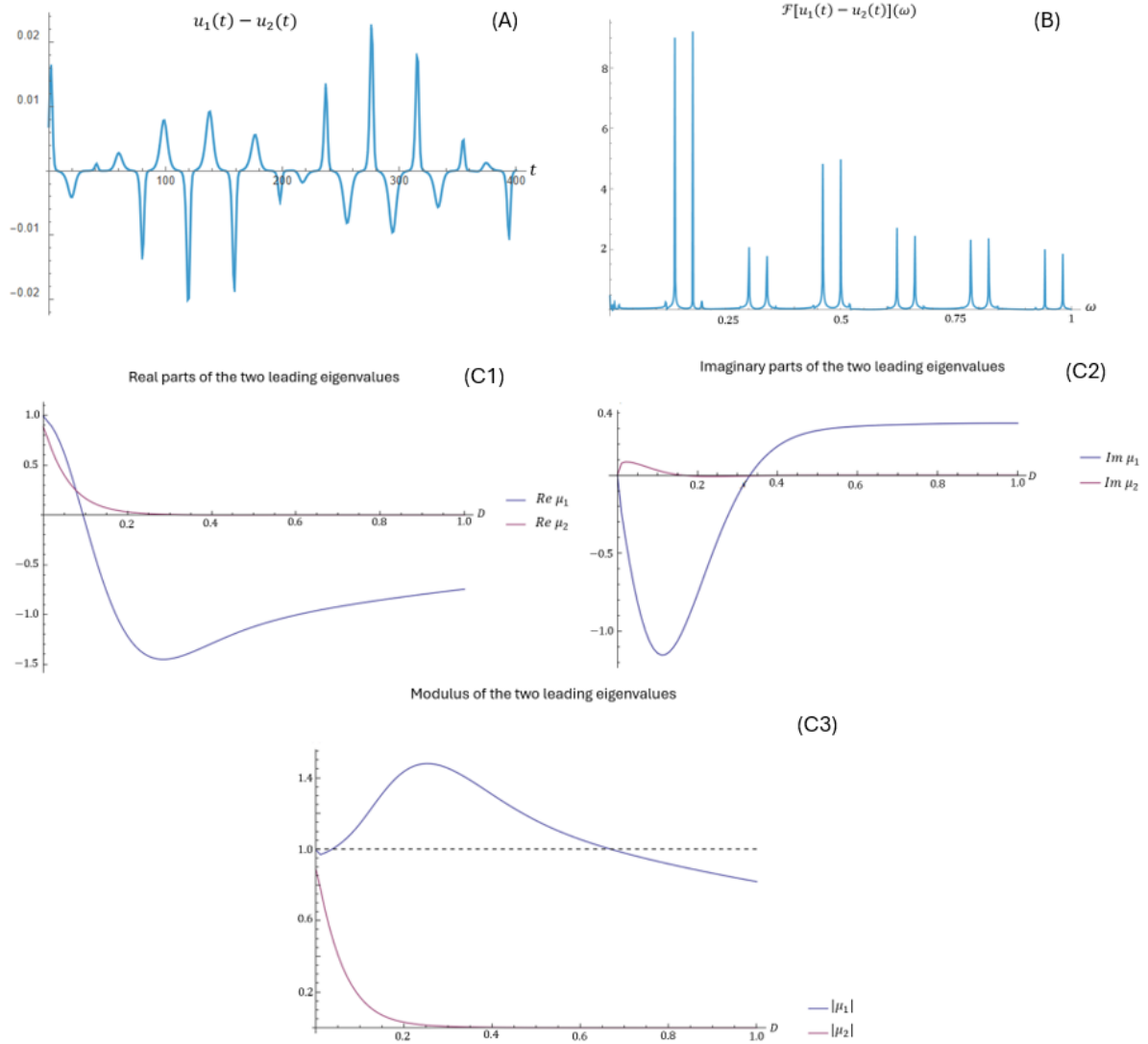


Figure 8: Quasi-periodic solution with the connectivity matrix C (shown below). The eigenvalues of C are $\{-\sqrt{2}, 0, e^{\pm i\pi/4}\}$. $D_u = 0.04$, $D_v = D_w = 0$.

$$C = \frac{1}{\sqrt{2}} \begin{pmatrix} -1 & 1 & 0 & 0 \\ 0 & -1 & 1 & 0 \\ 0 & 0 & -1 & 1 \\ 1 & 0 & 0 & -1 \end{pmatrix}$$

5 Master stability function

In this section, we present the master-stability function (MSF) of system (23) with $\alpha = 2.3427, \gamma = 0.5, D_u = D, D_v = D_w = 0$. The stability of its periodic solution (24) was shown to be determined by the complex parameter $\Omega = D\lambda^s$, when λ^s are the eigenvalues of the connectivity matrix C , which can be chosen to be in the third quadrant. We calculate the Floquet multipliers of the linearized system

$$\begin{pmatrix} \dot{U}_j \\ \dot{V}_j \\ \dot{W}_j \end{pmatrix} = \begin{pmatrix} \Omega + \gamma - 2u_0(t) - \alpha v_0(t) & -\alpha u_0(t) & 0 \\ 0 & 1 - 2v_0(t) - \alpha w_0(t) & -\alpha v_0(t) \\ -\alpha w_0(t) & 0 & 1 - 2w_0(t) - \alpha u_0(t) \end{pmatrix} \begin{pmatrix} U_j \\ V_j \\ W_j \end{pmatrix} \quad (41)$$

and check for which Ω the largest Floquet multiplier is less than 1. Define $\Omega = -Re^{i\theta}, 0 \leq \theta < \frac{\pi}{2}$. If we fix θ , and look at the instability region in R , we find that for sufficiently small θ the instability region is an interval in R . If we denote I_θ as the instability interval, we see that for $\theta_1 < \theta_2$ $I_{\theta_1} \subset I_{\theta_2}$. For $\theta > \frac{2}{5}\pi$, more than one instability interval is possible and the inclusion property above no longer holds. We saw that for $R > 1.2$, there is stability for every θ . The complete master-stability function is shown in Figure 9.

At small $|\Omega|$, the multiplier μ_1 can be presented as:

$$\mu_1(\Omega) = 1 + \mu_1^{(1)}\Omega + \mu_1^{(2)}\Omega^2 + o(\Omega^2),$$

where $\mu_1^{(1)} > 0, \mu_1^{(2)} < 0$. For $\Omega = -R \exp(i\theta)$, we get

$$\mu_1(R, \theta) = 1 - \mu_1^{(1)}R \cos \theta + \mu_1^{(2)}R^2 \cos 2\theta + i(-\mu_1^{(1)}R \sin \theta + \mu_1^{(2)}R^2 \sin 2\theta) + o(R^2).$$

Therefore,

$$|\mu_1(R, \theta)|^2 = 1 - 2\mu_1^{(1)}R \cos \theta + (\mu_1^{(1)2} + 2\mu_1^{(2)} \cos 2\theta)R^2 + o(R^2).$$

Calculating the coefficients $\mu_1^{(1)}, \mu_1^{(2)}$ gives: $\mu_1^{(1)} = 35.7, \mu_1^{(2)} = -5.8 \cdot 10^3$. Note that $\mu_1^{(1)}/|\mu_1^{(2)}| \sim 10^{-4}$. Therefore, for $R > 10^{-2}$, the terms with $\mu_1^{(1)}$ in the expression for $|\mu_1|^2$ are negligible. If the terms containing $\mu_1^{(1)}$ are disregarded, one finds that the solution is stable for small R in the region $\theta < \pi/4$ and unstable in the region $\theta > \pi/4$; this prediction is confirmed by numerical computations (see Figure 9(A)). However, for $\theta > \pi/4$, the solution is actually stable in a very short, invisible on the plot, interval $0 \leq R \leq R_*$, where $R_* \approx 2\mu_1^{(1)} \cos \theta / (2\mu_1^{(2)} \cos 2\theta + \mu_1^{(1)2})$.

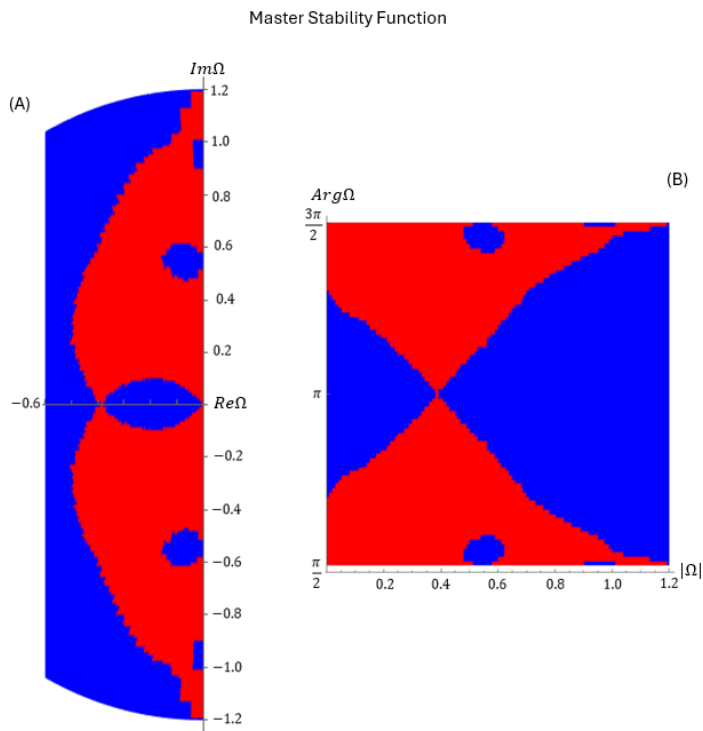


Figure 9: Master-Stability function of (23) with $\alpha = 2.3427, \gamma = 0.5, D_v = D_w = 0$ with respect to the stability parameter $\Omega = D\lambda^s$. The red regions are corresponding to the points for which the leading Floquet multiplier is greater than one (i.e instability), and the blue regions are corresponding to the case where the leading Floquet multiplier is less than one (stability). The left graph (A) is the MSF in cartesian coordinates, $(Re\Omega, Im\Omega)$, and the right graph (B) is the MSF in polar coordinates, $(|\Omega|, Arg\Omega)$.

6 Conclusion

In this paper, we analyze the stability of synchronous oscillations in networks of coupled, strongly nonlinear oscillators, using the three-species Lotka–Volterra system as an illustration. We established explicit conditions under which the loss of stability of synchronous oscillations in a network is equivalent to the modulational instability of the uniform oscillation in a reaction-diffusion medium, via the spectral correspondence $D_i \lambda^s \leftrightarrow -d_i k^2$. For undirected couplings (real spectra) this yields a one-to-one mapping between finite wavenumber instability bands and finite coupling intervals; for directed couplings (complex spectra) stability is characterized by the master-stability function (MSF) in the complex plane. Using the properties of Metzler and standardized Laplacian matrices, we obtained a practical criterion for detecting the onset of desynchronization and, leveraging Floquet analysis, computed the MSF. The computations reveal alternating parameter windows of synchronization and desynchronization (intermittency) in the three-species model, with re-stabilization at sufficiently weak and sufficiently strong coupling. These results delineate parameter regimes that support synchrony and provide tools transferable to other multi-species networks.

A Derivation for more general linear operators

Let us look at the more general problem:

$$\dot{u} = f(u) + L[u] \quad (42)$$

where u is an n -component vector function depending on variables t and x , f is a smooth, generally nonlinear, function, and $L[u]$ is a linear differential operator,

$$(L[u])_s = \sum_{j=1}^n a_{sj} \frac{\partial^j u_s}{\partial x^j},$$

where a_{sj} are constant coefficients. We aim to check the stability of a solution $u_0(t)$ of the non-spatial problem: $\dot{u} = f(u)$ with respect to the perturbations: $u(x, t) = u_0(t) + \epsilon U(t) e^{ikx}$, $0 < \epsilon \ll 1$. Substituting this solution into (42) and considering only the components of $O(\epsilon)$ yields the following:

$$\dot{U} = J|_{u=u_0(t)} U + L[e^{ikx}]U \quad (43)$$

where J is the Jacobi matrix of f , and $U(t)$ is generally complex. Equation (43) is a vector equation. For each component U^s , the equation looks as follows:

$$\dot{U}^{(s)} = J^{(s)}|_{u=u_0(t)} U^{(s)} + \sum_{j=1}^n a_j^{(s)} (ik)^j U^{(s)} \quad (44)$$

This equation is equivalent to equation (13) with $D_i \lambda^s = \sum_{j=1}^n a_j^{(s)} (ik)^j$, and the stability analysis is similar to that shown in 2.3.

In the more general case, for every $g : \mathbb{R}^n \rightarrow \mathbb{C}^n$ that has a Fourier transform, one can use the operator: $(L[u])_s = \int_{-\infty}^{\infty} g^{(s)}(x-y) u_s(y) dy = (g^{(s)} * u_s)(x)$. After substituting the perturbative solution within the integral, one obtains the linear equation, which is equivalent to (13) with $D_i \lambda^s = \hat{g}^{(s)}(k)$.

References

- [1] M. Argentina, P. Coullet, and E. Risler, Self-parametric instability in spatially extended systems, *Phys. Rev. Lett.* **86** (2001) 807–809.
- [2] I. Sorin, A. Nepomnyashchy, and V. Volpert, “Stability of oscillations in the spatially extended May–Leonard model,” *arXiv preprint arXiv:2502.18048*, 2025.
- [3] R. M. May and W. J. Leonard, “Nonlinear aspects of competition between three species,” *SIAM J. Appl. Math.*, vol. 29, pp. 243–253, 1975.
- [4] A. Pikovsky and A. Politi, *Lyapunov Exponents: A Tool to Explore Complex Dynamics*, Cambridge University Press, 2016.
- [5] H. Nakao and A. S. Mikhailov, “Turing patterns in network-organized activator–inhibitor systems,” *Nature Physics*, 2010.
- [6] A. Cvetković, “Stabilising the Metzler matrices with applications to dynamical systems,” *arXiv preprint arXiv:1901.05522*, 2019.
- [7] S. A. Gershgorin, Über die Abgrenzung der Eigenwerte einer Matrix, *Izv. Akad. Nauk SSSR, Otd. Fiz.-Mat. Nauk* **6** (1931) 749–754.
- [8] R. P. Agaev and P. Yu. Chebotarev, *On the spectra of nonsymmetric Laplacian matrices*, Linear Algebra and its Applications **399** (2005), 157–168.
- [9] R. S. Cantrell and C. Cosner, *Spatial Ecology via Reaction–Diffusion Equations*, Wiley Series in Mathematical and Computational Biology, Wiley, 2003.
- [10] J. Coste, J. Peyraud, and P. Coullet, “Asymptotic behaviors in the dynamics of competing species,” *SIAM J. Appl. Math.*, vol. 36, no. 3, pp. 516–528, 1979.
- [11] C.-W. Chi, S.-B. Hsu, and L.-I. Wu, “On the asymmetric May–Leonard model of three competing species,” *SIAM J. Appl. Math.*, vol. 58, pp. 211–226, 1998.
- [12] I. Sorin, M. Zaks, and A. Nepomnyashchy, “Seasonal Forcing in Rock–Paper–Scissors Population Dynamics”, preprint.
- [13] C. M. Postlethwaite and A. M. Ruckridge, “Stability of cycling behaviour near a heteroclinic network model of Rock–Paper–Scissors–Lizard–Spock,” *Nonlinearity*, vol. 35, no. 4, pp. 1702–1733, 2022.
- [14] A. Pikovsky and A. Nepomnyashchy, “Chaos in coupled heteroclinic cycles and its piecewise-constant representation,” *Physica D: Nonlinear Phenomena*, vol. 452, pp. 133772, 2023.
- [15] A. Bayliss, A. A. Nepomnyashchy, and V. A. Volpert, “Beyond rock–paper–scissors systems—Deterministic models of cyclic ecological systems with more than three species,” *Physica D: Nonlinear Phenomena*, vol. 411, pp. 132585, 2020.
- [16] S. Ehrich, A. Pikovsky, and M. Rosenblum, “From complete to modulated synchrony in networks of identical Hindmarsh–Rose neurons,” *Eur. Phys. J. Special Topics*, vol. 222, pp. 2407–2416, 2013.